Charge excitations in cuprate and nickelate in resonant inelastic x-ray scattering

2009 J. Phys.: Condens. Matter 21 064236

(http://iopscience.iop.org/0953-8984/21/6/064236)

IOP PUBLISHING JOURNAL OF PHYSICS: CONDENSED MATTER

J. Phys.: Condens. Matter **21** (2009) 064236 (6pp) doi:10.1088/0953-8984/21/6/064236

Charge excitations in cuprate and nickelate in resonant inelastic x-ray scattering

Manabu Takahashi[1], **Jun-ichi Igarashi**[2] **and Taeko Semba**[2]

[1] Faculty of Engineering, Gunma University, Kiryu, Gunma 376-8515, Japan
[2] Faculty of Science, Ibaraki University, Mito, Ibaraki 310-8512, Japan

Received 19 July 2008, in final form 29 July 2008
Published 20 January 2009
Online at stacks.iop.org/JPhysCM/21/064236

Abstract

We analyze the resonant inelastic x-ray scattering (RIXS) spectra at the Cu and Ni K-edges in La_2CuO_4 and La_2NiO_4, respectively. We make use of the Keldysh–Green function formalism, in which the RIXS intensity is described by a product of the incident-photon-dependent factor and the density–density correlation function in the 3d states. The former factor is calculated using the 4p density of states given by an *ab initio* band structure calculation and the latter using the wavefunctions given by a Hartree–Fock calculation of a multiorbital tight-binding model. The initial state is described within the Hartree–Fock approximation and the electron correlations on charge excitations are treated within the random phase approximation. The calculated RIXS spectra reproduce well several characteristic features in the experiments. Although several groups have interpreted the RIXS peaks as bound excitons, our calculation indicates that they should be interpreted as band-to-band excitations augmented by electron correlations. The difference in RIXS spectra between La_2CuO_4 and La_2NiO_4 is explained from this point of view.

1. Introduction

Investigation of the electronic excitations in the transition metal compounds is fundamental for understanding their electronic properties. The excitations may be characterized into two types, spin and charge excitations. For the former, the inelastic neutron scattering technique is quite useful to investigate energy–momentum relations. For the latter, taking advantage of strong synchrotron sources, the resonant inelastic x-ray scattering (RIXS) technique has become a powerful tool to probe charge excitations and to investigate their energy–momentum relations. For the RIXS tuned at the transition metal K-edge, the process is described as a second-order optical process, in which a 1s core electron is excited to an empty 4p state by absorbing a photon, then charge excitations are created in the 3d states to screen the core–hole potential, and finally the photoexcited 4p electron recombines with the 1s core hole by emitting a photon. In the end, the charge excitations are left behind.

RIXS measurement at the Cu K-edge has been carried out to search for charge excitation modes and to determine the momentum dependence of charge excitation in high T_C cuprates and their related materials for a better understanding of the unconventional high-T_C superconductivity. For the undoped material La_2CuO_4, the RIXS spectra as a function of energy loss are composed of several peaks and show clear momentum dependence [1–4]. The peak position in terms of energy loss shifts remarkably as the momentum transfer changes. Several groups have claimed that the RIXS intensity reflects a bound exciton and interpreted the peak shifts as a dispersion relation of a bound exciton [4, 5]. The RIXS experiment at Ni K-edge on La_2NiO_4, which is isostructural with La_2CuO_4, has also been carried out in order to clarify the difference in charge excitations from La_2CuO_4. In contrast to the cuprate, no superconductivity has been reported in the nickelate. It has been reported that the RIXS spectra are composed of several peaks which do not show clear momentum dependence. The peak position in terms of energy loss does not shift even though the momentum transfer varies. It has been suggested that the exciton is well localized in the nickelate, while it is mobile in the cuprate [4].

On the other hand, it has been argued that the RIXS intensity should be interpreted as band-to-band excitations augmented by electron correlations, not as bound excitons.

Nomura and Igarashi (NI) [6, 7] have proposed a general formalism of the RIXS spectra by extending the resonant Raman theory developed by Nozières and Abrahams [8] on the basis of the many-body formalism of Keldysh. In the NI formula, with the assistance of the Born approximation on the interaction between the 1s hole and 3d electrons, the RIXS intensity is described by a product of an incident-photon-dependent factor and a density–density correlation function in the 3d states. The NI formula has been successfully applied to the quasi-one-dimensional cuprates $SrCuO_3$ [6] and $CuGeO_3$ [9], two-dimensional cuprate La_2CuO_4 [7, 10, 11] and the prototypical AFM insulator NiO [12]. In these studies, the electronic structures in the AFM phase have been calculated within the Hartree–Fock approximation (HFA) using tight-binding models. It is known that the HFA works well for describing the electronic structures in the AFM insulators. Two-particle correlations have been taken into account within the random phase approximation (RPA), which has been found to modify the spectral shape as a function of energy loss, having led to a good agreement with the experiments. On the basis of these successes, we may conclude that the RIXS intensity arises from band-to-band transitions to screen the core–hole potential in the intermediate state. Multiple-scattering contributions due to the core–hole potential have also been investigated in order to examine the validity of the Born approximation, because the core–hole potential is definitely not weak. Having evaluated the contributions by means of the time-representation method by Nozières and De Dominicis [13], it was found that the contributions could be mainly absorbed into the shift of the core-level energy with minor modifications of the RIXS spectral shape [10]. This result partly justifies the use of the Born approximation.

In the present study, we discuss the RIXS intensity and clarify the origin of the difference in it in La_2CuO_4 and La_2NiO_4 by applying the NI formula. We exploit the tight-binding HFA calculation and the *ab initio* band structure calculation based on the local density approximation(LDA) to calculate the density–density correlation function and the incident-photon-dependent factor, respectively. We obtain a stable AFM insulating solution having an energy gap of about 1.7 (3.5) eV within the HFA for La_2CuO_4 (La_2NiO_4). Note that the band structure calculation with the LDA fails to describe the AFM insulating state for these systems. The two-particle correlations in the intermediate states are treated within the RPA. We obtain the RIXS intensities in a range of energy loss 2–6 (4–8) eV for La_2CuO_4 (La_2NiO_4). The calculated RIXS spectra reproduce well several characteristic features in the experiments [2–4]. In particular, the calculated RIXS spectra for La_2CuO_4 exhibit a noticeable momentum dependence of the peak structure while those for La_2NiO_4 only do so slightly, being consistent with the experiments. Although our results do not reproduce all features in the RIXS spectra at this stage partly because of the strong correlation between 3d electrons, our results suggest that the RIXS intensity should be interpreted as a band-to-band transition and the peak shifts as a function of momentum should not be interpreted as a dispersion relation of a kind of exciton, because the peaks with broad width constitute an energy continuum generated by a band-to-band transition.

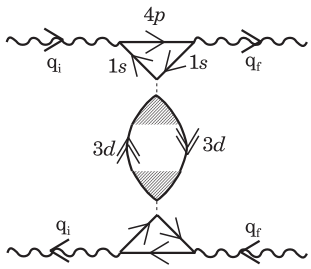

Figure 1. Diagrammatic representation for the RIXS intensity. The wavy and solid lines represent photon and electron bare Green functions, respectively. The dotted line is the core–hole interaction V. The solid lines with double arrows are the Keldysh-type Green functions. The shaded area represents the effective scattering vertex renormalized by 3d–3d Coulomb interaction in the RPA.

The present paper is organized as follows. In section 2, we briefly summarize the NI formula for the RIXS spectra. In section 3 we discuss the calculated RIXS spectra comparing with the experiments in connection with the electronic structure within the HFA in the AFM phase of La_2CuO_4 and La_2NiO_4. The last section is devoted to the concluding remarks.

2. RIXS formula

We briefly summarize the NI formula for the RIXS. In the RIXS process, an incident photon is absorbed by exciting a Cu (Ni) 1s core electron to the unoccupied Cu (Ni) 4p state, and a photon is emitted by recombining the 4p electron and the core hole. In the intermediate state of the RIXS process, the core–hole potential acts on the 3d states and creates electron–hole pairs in order to screen the core–hole potential. In the end of the process, a single electron–hole pair is left behind within the Born approximation, carrying momentum–energy $q \equiv (\mathbf{q}, \omega) = (\mathbf{q}_i - \mathbf{q}_f, \omega_i - \omega_f)$, where $q_i = (\mathbf{q}_i, \omega_i)$ and $q_f = (\mathbf{q}_f, \omega_f)$ are the momentum–energy of incident and scattered photons, respectively. The RIXS intensity is derived on the basis of the Keldysh–Green function scheme. The process is diagrammatically shown in figure 1. Within the Born approximation to the core–hole potential, the RIXS intensity is given by

$$W(q_i, \mathbf{e}_i; q_f, \mathbf{e}_f) = \frac{N\,|w|^4}{4\omega_i\omega_f} \times \sum_{\lambda m\sigma}\sum_{\lambda' m'\sigma'} Y^{+-}_{\lambda m\sigma,\lambda' m'\sigma'}(q)\, J_{\mathrm{B}\lambda\lambda'}\left(\omega_i, \mathbf{e}_i; \omega_f, \mathbf{e}_f\right), \qquad (1)$$

where λ indicates the Cu (Ni) site λ in a unit cell. N is the number of the unit cell and w is the 1s–4p dipole transition matrix element, which is assumed to be constant. The factor $J_{\mathrm{B}\lambda\lambda'}(\omega_i, \mathbf{e}_i; \omega_f, \mathbf{e}_f)$ describes the incident photon dependence, which is given by

$$J_{\mathrm{B}\lambda\lambda'}\left(\omega_i, \mathbf{e}_i; \omega_f, \mathbf{e}_f\right) = \left(\sum_{\eta\eta'} e_{i\eta} L^{\eta\eta'}_{\mathrm{B}\lambda}\left(\omega_i; \omega_f\right) e_{f\eta'}\right) \times \left(\sum_{\eta\eta'} e_{i\eta} L^{\eta\eta'}_{\mathrm{B}\lambda'}\left(\omega_i; \omega_f\right) e_{f\eta'}\right)^*, \qquad (2)$$

where $e_{i\eta}$ ($e_{f\eta}$) is the η component of the polarization vector $\mathbf{e}_i$ ($\mathbf{e}_f$) with $\eta = x, y, z$, and $L^{\eta\eta'}_{\mathrm{B}\lambda}(\omega_i; \omega_f)$ is given by

$$L^{\eta\eta'}_{\mathrm{B}\lambda}(\omega_i; \omega_f) = \frac{V}{N} \times \int_{\epsilon_0}^{\infty} \frac{\rho^{\eta\eta'}_{\lambda 4\mathrm{p}}(\epsilon)\, \mathrm{d}\epsilon}{(\omega_i + \epsilon_{1\mathrm{s}} + i\Gamma_{1\mathrm{s}} - \epsilon)(\omega_f + \epsilon_{1\mathrm{s}} + i\Gamma_{1\mathrm{s}} - \epsilon)}. \quad (3)$$

V represents the 1s core–hole potential acting on the 3d electrons, $\Gamma_{1\mathrm{s}}$ is the lifetime broadening width of the core–hole state and the lower limit of the integral ϵ_0 indicates the energy at the bottom of the conduction band. This expression comes from the upper triangle in figure 1. The $\rho^{\eta\eta'}_{\lambda 4\mathrm{p}}$ is the DOS matrix in the p symmetric states at the Cu (Ni) site λ, which may be given by

$$\rho^{\eta\eta'}_{\lambda 4\mathrm{p}}(\epsilon) = \sum_{\sigma} \sum_{n\mathbf{k}} \phi^{*}_{\lambda\eta\sigma}(n, \mathbf{k})\, \phi_{\lambda\eta'\sigma}(n, \mathbf{k})\, \delta(\epsilon - \epsilon_n(\mathbf{k})), \quad (4)$$

where $\phi_{\lambda\eta\sigma}(n, \mathbf{k})$ is the amplitude of the p_η component with spin σ at the Cu (Ni) site λ in the band state specified by the band index n and momentum $\mathbf{k}$ with energy $\epsilon_n(\mathbf{k})$. The factor $Y^{+-}_{\lambda' m'\sigma', \lambda m\sigma}(q)$ in equation (1) is the density–density correlation function of the Keldysh type, which is defined by

$$Y^{+-}_{\lambda' m'\sigma', \lambda m\sigma}(\mathbf{q}, \omega) = \int_{-\infty}^{\infty} \langle (\rho_{\mathbf{q}\lambda' m'\sigma'})^{\dagger}(\tau) \rho_{\mathbf{q}\lambda m\sigma}(0) \rangle \mathrm{e}^{\mathrm{i}\omega\tau}\, \mathrm{d}\tau, \quad (5)$$

where

$$\rho_{\mathbf{q}\lambda m\sigma} = \sqrt{\frac{1}{N}} \sum_{\mathbf{k}} d^{\dagger}_{\mathbf{k}+\mathbf{q}\lambda m\sigma} d_{\mathbf{k}\lambda m\sigma}, \quad (6)$$

with

$$d_{\mathbf{k}\lambda m\sigma} = \sqrt{\frac{1}{N}} \sum_{n} d_{n\lambda m\sigma} \mathrm{e}^{\mathrm{i}\mathbf{k}\cdot(\mathbf{r}_n + \mathbf{u}_\lambda)}. \quad (7)$$

$d_{\mathbf{k}\lambda m\sigma}$ is an annihilation operator for the state denoted by the index $\mathbf{k}\lambda m\sigma$. The index $\lambda m\sigma$ specifies a tight-binding orbital at the Cu (Ni) site λ with 3d orbital m and spin σ. The wavevector $\mathbf{k}$ in equation (6) runs over the first Brillouin zone. Vectors $\mathbf{r}_n$ and $\mathbf{u}_\lambda$ in equation (7) represent a position vector of the nth unit cell and the position vectors of the Cu (Ni) site λ in the unit cell n.

We calculate the density–density correlation function (5) by taking account of the correlation effect on the electron–hole pair by the RPA as shown in figure 1. For more details of the derivation, see [10–12].

3. Results and discussion

In order to calculate the incident-photon-dependent factor $J_{\mathrm{B}\lambda\lambda'}(\omega_i, \mathbf{e}_i; \omega_f, \mathbf{e}_f)$, we need the 4p DOS $\rho^{\eta\eta'}_{\lambda 4\mathrm{p}}(\epsilon)$ on the Cu (Ni) site λ. We use the 4p DOS given by the band structure calculation based on the LDA, assuming nonmagnetic states. Although the LDA fails to describe the antiferromagnetic insulating states with a wide energy gap, the calculated 4p DOS in the conduction band may be reliable because the 4p DOS has large intensity in the energy range above about 10 eV higher than the top of the occupied states. Due to the crystal symmetry, $\rho^{\eta\eta'}_{\lambda 4\mathrm{p}}(\epsilon)$ is almost independent of the Cu (Ni) site

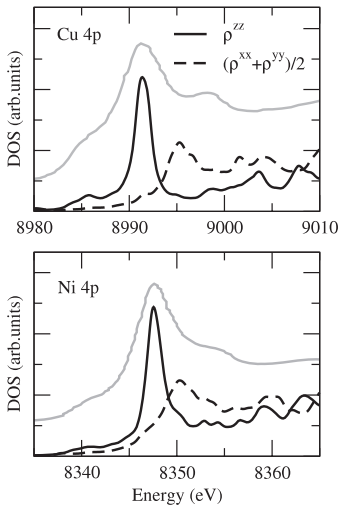

Figure 2. $\rho^{zz}_{\lambda 4\mathrm{p}}$ and $(\rho^{xx}_{\lambda 4\mathrm{p}} + \rho^{xx}_{\lambda 4\mathrm{p}})/2$ at the Cu and Ni site λ comparing with the fluorescence yield (gray solid curve) reproduced from [4]. Energy zero of the DOS is shifted so that the energy of the prominent peak in ρ^{zz} coincides with the fluorescence peak.

λ, $\rho^{xx}_{\lambda 4\mathrm{p}}(\epsilon) \approx \rho^{yy}_{\lambda 4\mathrm{p}}(\epsilon) \neq \rho^{zz}_{\lambda 4\mathrm{p}}(\epsilon)$, and the values for $\eta \neq \eta'$ are negligible. We set the energy difference between the Cu (Ni) 1s level and the prominent peak in $\rho^{zz}_{\lambda 4\mathrm{p}}(\epsilon)$ to be 8992 (8348) eV, as shown in figure 2. Under the condition that the dipole matrix element is constant and that the interaction between the core hole and the 4p electron is neglected, the 4p DOS becomes proportional to the Cu (Ni) K-edge absorption spectra. In the following, we assume that the incident and emitted x-rays are polarized along the z direction. Accordingly, the factor $J_{\mathrm{B}\lambda\lambda'}(\omega_i, \mathbf{e}_i; \omega_f, \mathbf{e}_f)$ is replaced with the factor $|L^{zz}_{\mathrm{B}\lambda}(\omega_i; \omega_f)|^2$.

Another factor $Y^{+-}_{\lambda' m'\sigma, \lambda m\sigma}(q)$ mainly determines the structure of the RIXS spectra as a function of energy loss. We calculate this factor using the tight-binding wavefunction given by the HFA assuming the AFM order. The Cu (Ni) 3d orbitals, apical and in-plane O 2p orbitals are included in the tight-binding model. The Slater–Koster parameters are taken from the LAPW band structure calculation for La_2CuO_4 [14]. The same values are assumed for La_2NiO_4, because reliable Slater–Koster parameters are not available at this stage. Although a precise calculation based on first principles is strongly required, this assumption is plausible because the bond lengths Cu–O and Ni–O are nearly equal to each other [15, 16] and the band structures near the Fermi level calculated within the LDA assuming nonmagnetic states for La_2CuO_4 and La_2NiO_4 are similar to each other [17]. The intra-atomic Coulomb interaction on the Cu (Ni) sites is given by the Slater integrals F^0, F^2 and F^4. Among them, F^2 and F^4, which are known to be slightly screened by solid-state effects, are taken from the analysis of the x-ray photoemission spectroscopy [18, 19]. On the other hand, F^0 is known to be considerably screened, so that we regard the value as an adjustable parameter. The Coulomb interaction on O sites and that between Cu (Ni) 3d and O 2p orbitals are absorbed into a renormalization of the O 2p level parameters. The Cu (Ni) d level position relative to the O p levels is given by the charge-transfer energy Δ

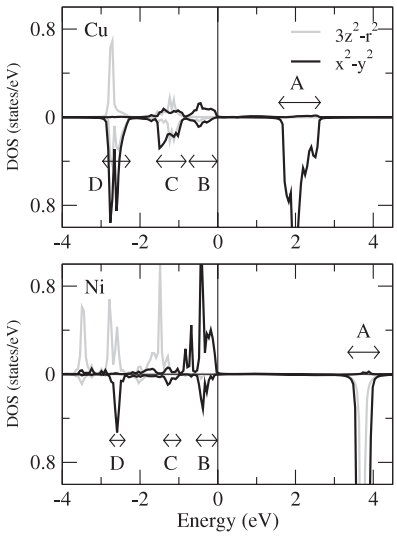

Figure 3. Partial DOS of $3z^2 - r^2$ and $x^2 - y^2$ orbital at a transition metal site and of the pσ orbital at an in-plane oxygen site for La_2CuO_4 (upper panel) and La_2NiO_4 (lower panel). Energy zero is at the top of the valence band. DOS for the local majority and the local minority spins are presented in the upper and lower half, respectively. Roman letters A, B, C and D are used to denote the energy ranges where the $x^2 - y^2$ partial DOS in the local minority spin has noticeable intensity.

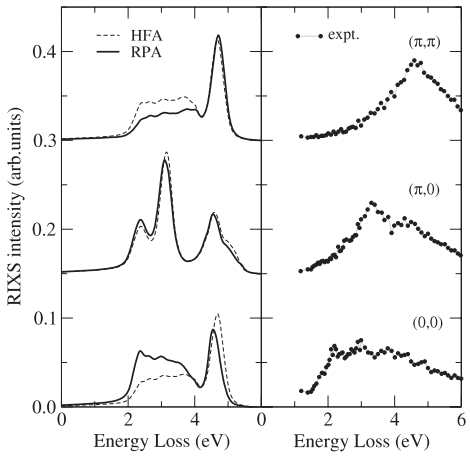

Figure 4. Calculated RIXS spectra (left) and experimental spectra (right) for La_2CuO_4. The experimental spectra are reproduced from [3]. Solid and dotted curves are the spectra calculated with RPA and HFA, respectively. Incident photon energy is assumed to be 8992 eV, although it is 8992.5 eV in the experiment.

defined as $\Delta = E_d - E_p + 9U$ ($\Delta = E_d - E_p + 8U$) in the d^9 (d^8) configuration for La_2CuO_4 (La_2NiO_4), where U is the multiplet-averaged d–d Coulomb interaction given by $U = F^0 - (2/63)F^2 - (2/63)F^4$ [20]. The charge-transfer energy Δ is also treated as an adjustable parameter in the present calculation. We assume $U = 11$ eV, $\Delta = 2.5$ eV ($U = 6$ eV, $\Delta = 4$ eV) for La_2CuO_4 (La_2NiO_4).

Figure 3 shows the DOS projected on the Cu (Ni) $3z^2 - r^2$ and $x^2 - y^2$ states. The calculated energy gap is about 1.7 (3.5) eV for La_2CuO_4 (La_2NiO_4). The $x^2 - y^2$ states of the local minority spin reside on both occupied and unoccupied energy regions with noticeable weight. Therefore, the transitions from the $x^2 - y^2$ states in the energy ranges denoted by B, C and D to the $x^2 - y^2$ states in the energy range denoted by A contribute to the screening process of the 1s core–hole potential and consequently to the RIXS intensity. We note that the transitions between the states having different local symmetry from each other is forbidden. The distribution of the $x^2 - y^2$ states of the local minority spin is similar between La_2CuO_4 and La_2NiO_4 except for the bandwidth. The bandwidth of the states including the $x^2 - y^2$ state of the local minority spin for La_2NiO_4 is much narrower than that of La_2CuO_4 due to the larger charge-transfer energy Δ. In La_2CuO_4, the $3z^2 - r^2$ states are completely occupied for both spins. In La_2NiO_4, a small amount of the $3z^2 - r^2$ states of the local minority spin reside even in the occupied energy region, while those of the local majority spin are completely occupied. Thus, the transition in the $3z^2 - r^2$ channel does not occur in La_2CuO_4, while the transition can contribute to the RIXS intensity in La_2NiO_4. In contrast to the e_g states, the t_{2g} states cannot contribute to the RIXS intensity, since the local majority and minority spin t_{2g} states are completely occupied.

Combining the two factors, we obtain the RIXS spectra by assuming the core–hole lifetime broadening $\Gamma_{1s} = 1$ eV. We convolute the result with a Lorentzian function of FWHM = 0.3 eV for taking account of the instrumental resolution. Figure 4 shows the calculated spectra for La_2CuO_4 at several momentum transfers $\mathbf{q}$ compared with experiment [3]. The RPA correction modifies the spectra calculated within HFA, leading to better agreement with the experiments. We obtain continuous spectra as a function of energy loss ω ranging from $\omega = 2$ to 6 eV. Intensities around $\omega = 2.2$, 3.2 and 4.5 eV are caused by charge excitations of $B \to A$, $C \to A$ and $D \to A$ transitions, respectively, within the $x^2 - y^2$ symmetry in the local minority spin states (see figure 3). A prominent peak around 4.5 eV stays at the same position with changing the momentum transfer $\mathbf{q}$. The spectral shape in the low energy region changes as the momentum transfer $\mathbf{q}$ varies. A broad hump existing around $\omega = 2$–4 eV at $\mathbf{q} = (0, 0)$, which is enhanced by the RPA correction, grows up to become a peak around 3.2 eV at $\mathbf{q} = (\pi, 0)$. This behavior corresponds well to the experimental lineshape at $\mathbf{q} = (\pi, 0)$, which looks like two peaks around $\omega = 3.2$ and 4.5 eV. On the other hand, the intensity of the broad hump around $\omega = 2$–4 eV is suppressed by the RPA correction at $\mathbf{q} = (\pi, \pi)$ and only one peak is overwhelmingly left at 4.5 eV. This explains the experimental spectra at $\mathbf{q} = (\pi, \pi)$, which looks like a single peak around $\omega = 4.5$ eV. Although several characteristic features of RIXS spectra are reproduced in good agreement with the experiments [3, 4], several discrepancies between the present calculation and the experiments still remain; the 4.5 eV peak is hardly discernible at $\mathbf{q} = (0, 0)$, while the intensity at $\omega = 4$ eV is large enough, forming a peak-like structure at $\mathbf{q} = (0, 0)$ with $\omega_i = 8992$ eV [2]. To remove these discrepancies, we may need to take account of the electron correlations beyond the RPA and the effects beyond the Born approximation to the core–hole potential.

Figure 5 shows the calculated spectra for La_2NiO_4 at several momentum transfers compared with experiment [4].

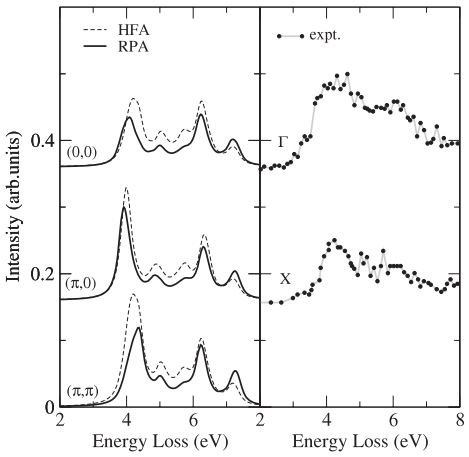

Figure 5. RIXS spectra for La_2NiO_4. The experimental spectra are reproduced from [4]. Incident photon energy is assumed to be 8348 eV.

We obtain continuous spectra ranging from $\omega = 4$ to 8 eV. The RPA correction works to suppress the spectra calculated within the HFA in a energy range 4–7 eV at all momentum transfers $\mathbf{q}$. The intensities around $\omega = 4$, 5 and 6.3 eV arise mainly from the charge excitations of B $\rightarrow$ A, C $\rightarrow$ A and D $\rightarrow$ A transitions, respectively, within the $x^2 - y^2$ symmetry in the local minority spin states. The transition between the $3z^2 - r^2$ states of the local minority spin also contributes to the intensity around $\omega = 5.8$ and 7.3 eV. In contrast to La_2CuO_4, the calculated RIXS spectra show only slight peak shifts and intensity changes as the momentum transfer $\mathbf{q}$ changes. This non-dispersive behavior of the peak structure as a function of energy loss is well consistent with the experiment [4]. We note that this is a consequence of the fact that the bandwidth of the $x^2 - y^2$ states of the local minority spin in La_2NiO_4 is much narrower than that in La_2CuO_4 due to the larger charge-transfer energy Δ.

4. Concluding remarks

We have analyzed the momentum transfer dependence of the RIXS spectra in La_2CuO_4 and La_2NiO_4 on the basis of the formula developed by Nomura and Igarashi. This formula expresses the RIXS spectra as a product of the density–density correlation function and the incident-photon-dependent factor. This formula makes it possible to calculate the RIXS spectra on the complicated models including many orbitals, and provide clear physical interpretations of the RIXS spectra. It may also be possible to incorporate this formula into an *ab initio* band structure calculation up to the RPA level, because the formula is similar to that of the dielectric function $\epsilon(\mathbf{q}, \omega)$. In the present study, a multiorbital tight-binding model, which includes all the Cu(Ni) 3d and O 2p orbitals as well as the full Coulomb interaction between 3d orbitals have been used to calculate the density–density correlation function, which has been calculated from the tight-binding wavefunctions within the HFA and RPA. The incident-photon-dependent factor has been evaluated from the 4p DOS given by the *ab initio* band structure calculation.

Our results reproduced several characteristic features in the RIXS experiments as a consequence of a band-to-band transition between the occupied and unoccupied $x^2 - y^2$ states of the local minority spin. The present calculation has also shown that in La_2NiO_4 the RIXS peak position in terms of energy loss shifts only slightly as the momentum transfer varies, while that looks to shift remarkably in La_2CuO_4, being consistent with the experiments. This is simply explained as a consequence of the fact that the bandwidth of the states contributing to the RIXS intensity is significantly narrower in La_2NiO_4 than in La_2CuO_4 because of a large charge-transfer energy Δ. The present calculation does not reproduce all features at this stage partly because of the strong correlation between 3d electrons. In spite of several drawbacks of our analysis, it is suggested that the peak shifts as a function of momentum should not be interpreted as a dispersion relation of a kind of exciton, because the peaks with broad widths constitute an energy continuum generated by a band-to-band transition. We have shown that the weight of the $x^2 - y^2$ states of the local minority spin in the occupied band states strongly depends on the momentum [11]. The momentum dependence of the weight of the $x^2 - y^2$ states of the local minority spin in the band states and the dispersion relation of the band states mainly determine the momentum transfer dependence of the RIXS intensity in the cuprate and nickelate.

Although experimental data have been accumulated for the doped cuprates and nickelates [4, 21–23], theoretical analyses are limited on a one-band Hubbard model within the exact diagonalization method [24], and on a three-band Hubbard model analysis within the HFA on the basis of the present formalism [25]. An analysis with a detailed model like the present paper may be necessary to clarify the momentum and incident photon dependence of the spectra. Since electron correlations are expected to be more important in the doped cuprates and nickelates, such studies seem rather hard and are left for the future.

Acknowledgments

This work was partly supported by a Grant-in-Aid for Scientific Research from the Ministry of Education, Culture, Sport, Science, and Technology, Japan.

References

[1] Kim Y J, Hill J P, Burns C A, Wakimoto S, Birgeneau R J, Casa D, Gog T and Venkataraman C T 2002 *Phys. Rev. Lett.* **89** 177003
[2] Lu L, Hancock J N, Chabot-Couture G, Ishii K, Vajk O P, Yu G, Mizuki J, Casa D, Gog T and Greven M 2006 *Phys. Rev.* B **74** 224509
[3] Ellis D S, Hill J P, Wakimoto S, Birgeneau R J, Casa D, Gog T and Kim Y-J 2008 *Phys. Rev.* B **77** 060501
[4] Collart E, Shukla Abhay, Rueff J-P, Leininger P, Ishii H, Jarrige I, Cai Y Q, Cheong S-W and Dhalenne G 2006 *Phys. Rev. Lett.* **96** 157004
[5] Zhang F C and Ng K K 1998 *Phys. Rev.* B **58** 13520
[6] Nomura T and Igarashi J-i 2004 *J. Phys. Soc. Japan* **73** 1677
[7] Nomura T and Igarashi J-i 2005 *Phys. Rev.* B **71** 035110
[8] Nozières P and Abrahams E 1974 *Phys. Rev.* B **10** 3099
[9] Suga S *et al* 2005 *Phys. Rev.* B **72** 081101

[10] Igarashi J-i, Nomura T and Takahashi M 2006 *Phys. Rev.* B **74** 245122
[11] Takahashi M, Igarashi J and Nomura T 2008 *J. Phys. Soc. Japan* **77** 034711
[12] Takahashi M, Igarashi J and Nomura T 2007 *Phys. Rev.* B **75** 235113
[13] Nozières P and De Dominicis C T 1969 *Phys. Rev.* **178** 1097
[14] DeWeert M J, Papaconstantopoulos D A and Pickett W E 1989 *Phys. Rev.* B **39** 4235
[15] Lander G H, Brown P J, Spal/ek J and Honig J M 1989 *Phys. Rev.* B **40** 4463
[16] Lander G H, Brown P J, Stassis C, Gopalan P, Spalek J and Honig G 1991 *Phys. Rev.* B **43** 448
[17] Mattheiss L F 1993 *Phys. Rev.* B **48** 4352
[18] Eskes H and Sawatzky G A 1991 *Phys. Rev.* B **43** 119
[19] Eisaki H, Uchida S, Mizokawa T, Namatame H, Fujimori A, van Elp J, Kuiper P, Sawatzky G A, Hosoya S and Katayama-Yoshida H 1992 *Phys. Rev.* B **45** 12513
[20] Bocquet A E, Mizokawa T, Saitoh T, Namatame H and Fujimori A 1992 *Phys. Rev.* B **46** 3771
[21] Ishii K *et al* 2005 *Phys. Rev. Lett.* **94** 187002
[22] Ishii K *et al* 2005 *Phys. Rev. Lett.* **94** 207003
[23] Lu L *et al* 2005 *Phys. Rev. Lett.* **95** 217003
[24] Tsutsui K, Tohyama T and Maekawa S 2003 *Phys. Rev. Lett.* **91** 117001
[25] Markiewicz R S and Bansil A 2006 *Phys. Rev. Lett.* **96** 107005